KOVAL'CHEK, V. M. & PEREKALINA, Z. B. (1972). *Sov. Phys. Crystallogr.* **17**, 355–356.

LIMINGA, R., ABRAHAMS, S. & BERNSTEIN, J. L. (1980). *J. Chem. Phys.* **73**(3), 1432–1438.

MELLOR, J. W. (1957). *A Comprehensive Treatise on Inorganic and Theoretical Chemistry*, Vol. 10, 576–590. New York: Longmans, Green.

RAUSELL-COLLONE, J. A. & GARCIA-BLANCO, S. (1966). *Acta Cryst.* **21**, 672–675.

SILKER, T. R. (1964). *J. Opt. Soc. Am.* **11**, 1348–1351.

STANLEY, E. (1956). *Acta Cryst.* **9**, 897–900.

WATKIN, D. J., CARRUTHERS, J. R. & BETTERIDGE, P. W. (1985). *CRYSTALS User Guide*. Chemical Crystallography Department, Univ. of Oxford, England.

A New Approach to Describing Non-Molecular Crystal Structures

BY A. VEGAS, A. ROMERO AND M. MARTÍNEZ-RIPOLL

Instituto Rocasolano-CSIC, UEI de Cristalografía, Serrano 119, E-28006 Madrid, Spain

Abstract

A new model which relates the structure of a given compound to that of the parent metal is reported. The structures of oxides are regarded as the metal structure, sometimes deformed, sometimes opened up by the inclusion of other atoms, but maintaining the topology and interatomic distances of the parent metal structure. The model describes all the Mg-containing borates and silicates of the humite and leucophoenicite series as derived from their common parent h.c.p. Mg structure. The cation array of apatite and the alloy Ca_2Si are also analyzed in terms of the structures of elemental calcium.

Introduction

It is well known that the traditional ionic model assumes the existence of close-packed anion arrays (normally h.c.p. or f.c.c.), with small cations inserted into the octahedral and/or tetrahedral interstices. Location of cations in one of these holes, and hence the coordination number of the cation, is determined by the radius ratio (r^+/r^-). Consequently, inorganic crystal structures have been described as being formed by such interconnected polyhedra. This approach, although widely used to describe and understand inorganic crystal structures, cannot be generally applied and many 'complicated' structures do not find any satisfactory explanation in terms of this model. Obvious failures have been pointed out by Hyde (1986).

An alternative model, with the emphasis placed on the cation arrays, has been proposed by O'Keeffe & Hyde (1981, 1985), in which cation–cation repulsions and the coordination number of anions by cations are considered to be responsible for determining a given structure, the size of a cation being quantified by the so-called 'non-bonding radius' (O'Keeffe & Hyde, 1981). An additional feature observed by these authors is that, in many oxides and fluorides, the cation arrays are more regular than those of anions and that they have the structure of either elements or simple alloys. Thus, in TiO_2 (rutile), the Ti atom arrangement is that of the tetragonal body-centered β-Hg. In forsterite (Mg_2SiO_4), the Mg_2Si array is that of the Ni_2In alloy. Further, the structure of Si is maintained in cristobalite (SiO_2). In view of this, the structures could be better described as 'anion-stuffed alloys', which are the inverse of the traditional ionic model (cation-stuffed anion arrays). These principles were applied successfully to minerals, like the humite and the leucophoenicite families (White & Hyde, 1982*a,b*, 1983), leading to a simpler description of both structural families, and to a new structural relation between them that was not possible in terms of connected MO_6 octahedra (Belokoneva, Simonov & Belov, 1973). Application to other structure types was the subject of a further report (O'Keeffe & Hyde, 1985).

We think that this catonic approach represents an advance in both description and explanation of crystal structures, but unfortunately the crucial question, *i.e.* why a crystal structure has its actual structure and not another one, is far from being answered as yet. Even though the alternative model succeeds in many aspects not accounted for by the ionic model, we believe that some other considerations could be added. This is the aim of the present contribution.

Probably the most significant observation of O'Keeffe & Hyde (1985) is that in some oxides the cation arrangements are identical to those of the constituent elements, *i.e.* Si in high cristobalite SiO_2, Ca_2Si in β-Ca_2SiO_4, Y_5Si_3 in $Y_5(SiO_4)_3N$, Cu in

Cu_2O, Cu_3O_4 and CuO, BaS in high-temperature $BaSO_4$, *etc.* This has suggested the following questions to us: Why is a cation array, for example Mg_2Si in forsterite (Mg_2SiO_4), related to the Ni_2In alloy, a compound containing such different elements, and not to another A_2B-type alloy? Such a relation is very useful for descriptive purposes but it does not explain 'why' the actual structure is formed. Could it be possible, in some instances, to identify the original structure of the elements, even though not as clearly as it occurs in the examples cited above? In other words: Do the elements maintain their identity (structure), at least to some extent, when they are forming part of a compound? We attempt to answer these questions by examining the cation arrays of several compounds in the discussion below.

Discussion

Humite and leucophoenicite families

Hexagonal magnesium (h.c.p.) is the only known phase of this element, showing shortest Mg—Mg distances of 3·20 Å. We will show how the structural features of elemental Mg are preserved in all the compounds discussed below.

The cation arrays of the leucophoenicite family have been described (White & Hyde, 1982*a,b*, 1983; O'Keeffe & Hyde, 1985) as $(1,2^x)$ intergrowths of (1)CrB and (2)Ni_2In, with $x = 0, 1, 2, 3, \infty$ for CrB-type, $Mg_3(BO_3)_2$ (kotoite) (Zemann, Effenberger & Pertlik, 1982), $Mg_5(BO_3)_3F$ (Brovkin & Nikishova, 1975), $Mn_7(SiO_4)_3(OH)_2$ (leucophoenicite) and Mg_2SiO_4 (olivine) (Wenk & Raymond, 1973), respectively. In the humite series, the cations are ordered as $(2^x,3)$ intergrowths of (2)Ni_2In and (3)Re_3B, with $x = \infty, 3, 2, 1, 0$ for olivine, $Mg_9(SiO_4)_4(OH)_2$ (clinohumite) (Robinson, Gibbs & Ribbe, 1973), $Mg_7(SiO_4)_3(OH)_2$ (humite) (Ribbe & Gibbs, 1971), $Mg_5(SiO_4)(OH)_2$ (chondrodite) (Gibbs, Ribbe & Anderson, 1970) and $Mg_3(SiO_4)(OH)_2$ (norbergite) (Gibbs & Ribbe, 1969), respectively. The olivine, then, is the common structure which relates both families of compounds. Phases with $x > 3$ have also been identified by electron diffraction and high-resolution electron microscopy (White & Hyde, 1982*a,b*, 1983). In all of them, the resulting arrangement of the majority cation (say Mg or Mn) was described as a twinned f.c.c. packing, by reflection on $(113)_{fcc}$ planes. This twinning gives rise to (Si/B)-centered trigonal prisms of Mg which are common to all of the structures. Two features are worthy of mention: (i) no member of the leucophoenicite series is known to have the CrB arrangement, and (ii) no Mg-containing compound is known to have the leucophoenicite structure. For these reasons, the CrB alloy and leucophoenicite will not be discussed here. So far, we have used the interpretation of O'Keeffe & Hyde.

The structures of all these compounds are represented in Figs. 1(*a*) and 2(*a*), where it can be seen that, in the leucophoenicite series, all the Mg_6 trigonal prisms share edges and/or faces, so that their trigonal faces form infinite blocks. In the humite series however (Fig. 1), the trigonal faces of the prisms form isolated sets of one to four triangles for norbergite to clinohumite, respectively. However, a more detailed inspection of Fig. 1(*a*) reveals that the sets of triangles at the same height are separated by a distance close to that defining the triangular faces. Thus, the triangle sets, far from being isolated, can be considered as held together by additional Mg—Mg contacts like those represented by dashed lines in Fig. 1. In this way, in the humite series, the Mg_3 triangles also form infinite blocks in which the additional Mg—Mg contacts must be included. This is especially illustrative in the structure of norbergite (Fig. 1*a*) where isolated Mg_6Si trigonal prisms are depicted.

By comparing these sets of connected trigonal faces with the diagrams collected in Figs. 1(*b*) and 2(*b*), one can easily conclude that the former are merely fragments of closest packed sheets, as the $(001)_{hcp}$ or $(111)_{fcc}$. The trigonal faces of the prisms and the additional Mg—Mg contacts correspond to octahedral faces and edges, respectively, of such h.c.p. arrays. The diagrams represent h.c.p. arrays decomposed so as to reproduce the Mg patterns occurring in all the minerals we are dealing with. We note that all atoms of each h.c.p. array are involved in fragments of the same shape. Such a decomposition would also be possible for CrB and leucophoenicite and similar decompositions can also be achieved from f.c.c. packing, by reversing the sense of displacement in the C layer with respect to that applied in the A layer of an h.c.p.

The coincidence between the Mg blocks and the h.c.p. fragments is seen not only in the topology but also in the dimensions. The Mg—Mg distances (mean value 3·13 Å for olivine) compare quite well with that observed in metallic Mg (3·20 Å). Similar values are observed in all the other members of both families. Thus, the structures of all of these compounds can be regarded as fragments, different in size and shape, of the metallic structure of magnesium, which breaks down by inclusion of bulky SiO_4 tetrahedra. It is noteworthy that a greater Mg content corresponds to larger fragments of the parent element. In other words, the Mg atoms in the compounds are not distributed in an arbitrary way, but preserve their original arrangement as far as possible. This picture is far from that obtained when thinking in terms of the classical cation-centered polyhedra.

Returning to the earlier interpretation (O'Keeffe & Hyde, 1985), the twinned f.c.c. array of Mg atoms assigned to all these compounds seems to be an

implicit way of saying that a metallic elementary arrangement is present, even though this was not explicitly stated there. However, we believe that this is just an ideal representation, because a comparison of Mg—Mg distances with those in the unknown f.c.c. structure is not possible. Furthermore, the hypo- thetical $(113)_{fcc}$ planes are distorted, as demonstrated by the shortest Mg—Mg distances within the same $(113)_{fcc}$ plane, which are 4·75 Å in olivine. Unfortu- nately, we do not know the values of these distances in regular $(113)_{fcc}$ planes of the nonexistent f.c.c. Mg. On the contrary, what we do know is that the value
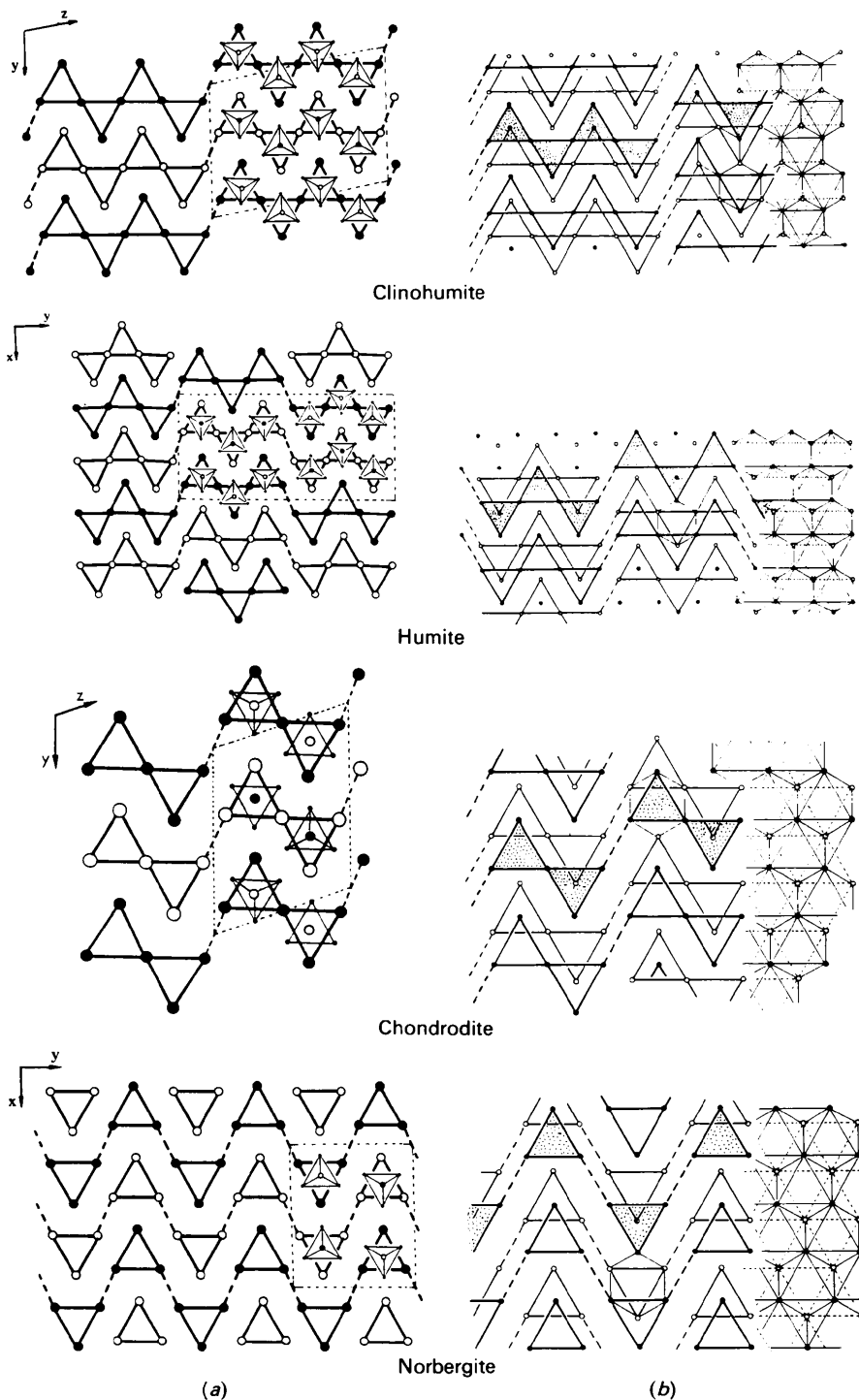

Clinohumite

Humite

Chondrodite

Norbergite

(a)   (b)

Fig. 1. The structures of the humite series. (a) Drawings of the structures showing the Mg_6 trigonal prisms projected onto their triangular faces and occu- pied by either SiO_4 tetrahedra or BO_3 triangles. The unit cell is marked. The Mg array has been extended out of the cell so as to show the sets of Mg_3 triangles joined by Mg—Mg contacts (dashed lines) forming infinite Mg blocks. Large circles rep- resent Mg atoms (open and filled atoms are shifted respect to each other by half of the pro- jection axes). (b) Set of Mg-like h.c.p. arrays decomposed so as to give the same blocks appearing in the corresponding mineral. In each diagram one of these blocks has been shaded. Dashed lines have the same meaning as in (a).

of 3·13 Å, found in the Mg_6 prisms, corresponds (within a few percent) to the octahedral edge of the existing h.c.p. Mg.

We believe that the discussion above provides a better representation of what could occur when a compound is formed. Conversely, one can also imagine how, in all cases, the parent structure (Mg) could be reconstructed if subtraction of the SiO_4 tetrahedra were possible!

Apatite and the structure of elemental calcium

Three phases of calcium are known, the f.c.c., h.c.p. and b.c.c. Two of them (h.c.p. and b.c.c.) can be recognized in apatite $Ca_5(PO_4)_3(OH,F)$. In the h.c.p. phase, the shortest Ca—Ca distance is 3·97 Å.

In the b.c.c. phase, the more significant Ca—Ca distances are: 3·88 Å (from the body center to the cube corners), 4·48 Å (the cube edges) and 6·33 Å (cube-face diagonals). A cube is equivalent to a flattened octahedron capped by two additional corners at two opposite triangular faces. When it is projected along the cube diagonal, the Ca flattened octahedron has horizontal edges of 6·33 Å and sloping edges of 4·48 Å.

The cation array of apatite (Sudarsanan & Young, 1978) is represented in Fig. 3(a). Its relation to Mn_5Si_3 was first observed by Schubert (1964) and by Wondratschek, Merker & Schubert (1964a,b). They described the Mn_5Si_3 structure as composed of both Mg-like and β-W-like blocks. Further, O'Keeffe & Hyde (1985) have described the structure of apatite

Kotoite $Mg_3(BO_3)_2$

$Mg_5(BO_3)_3F$

Olivine

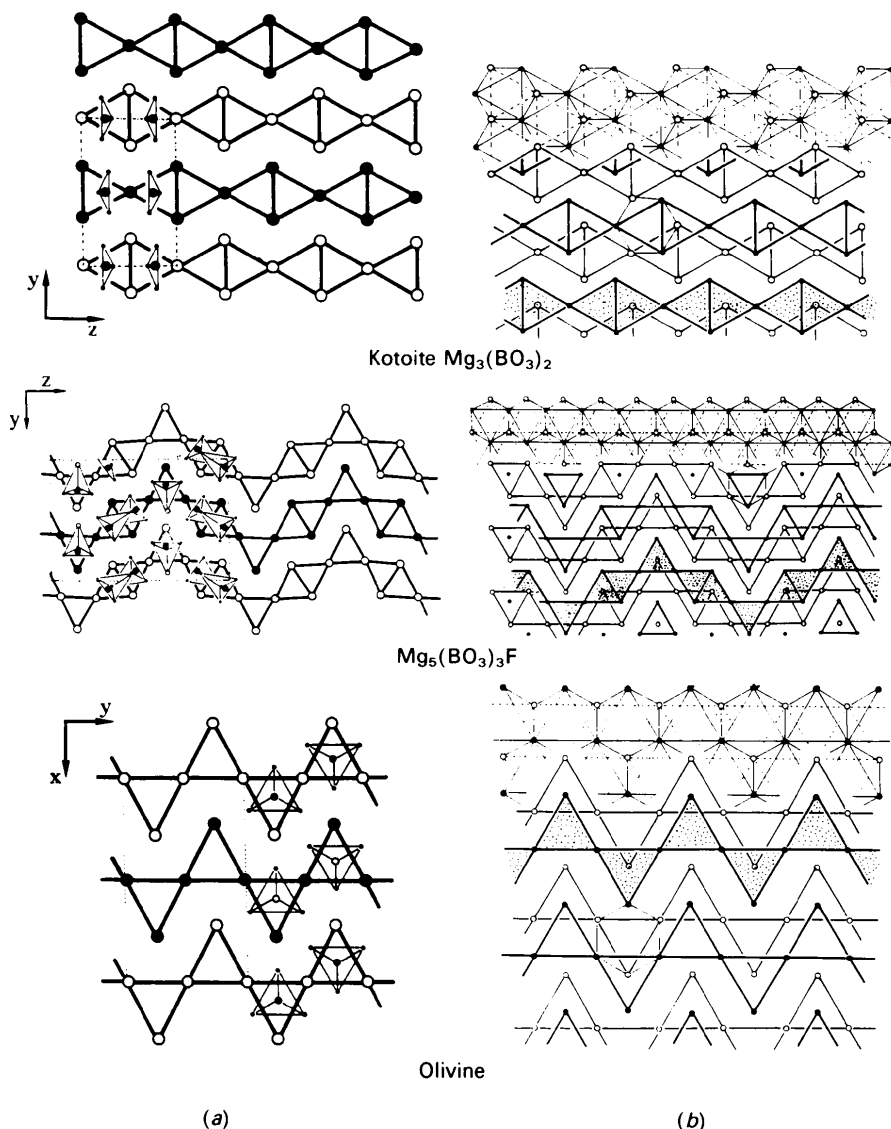(a)   (b)

Fig. 2. The structures of the leuco-phoenicite series. (a) and (b) have the same meaning as in Fig. 1. The Mg_6 trigonal prisms build infinite chains, so that no additional bonds (dashed lines) are needed.

as an oxygen-stuffed Ca_5P_3 array, following the model of Nyman & Andersson (1979) for the Mn_5Si_3 alloy, where only the h.c.p. blocks are recognized. This model, represents a simplification with respect to the classical description in terms of the cation-centered anion polyhedra. However, with respect to the cation array, we find it rather complicated, and for the following discussion we prefer the earlier description of Schubert (1964).

Considering only the Ca(1) atoms ($z = \frac{1}{4}, \frac{3}{4}$), the structure can be seen as a hexagonal packing, deformed by the inclusion of the PO_4 groups (Si, in Mn_5Si_3) into $Ca(1)_4$ tetrahedra, which are depicted in Fig. 3(a), so that regular and very deformed $Ca(1)_6$ octahedra alternate in the layers parallel to the xy plane. If the Ca(2) atoms are also considered, as they must be, the description is somewhat different. Two of them, at $z \simeq 0$, 1, cap the two horizontal faces of the deformed octahedron, and the third, at $z \simeq \frac{1}{2}$, lies at the body center. Thus, the whole can be seen as deformed b.c.c. blocks (the β-W blocks of Schubert) coexisting with the h.c.p. columns, running along the c axis of the hexagonal unit cell. Both polyhedra are represented in Fig. 3(b).
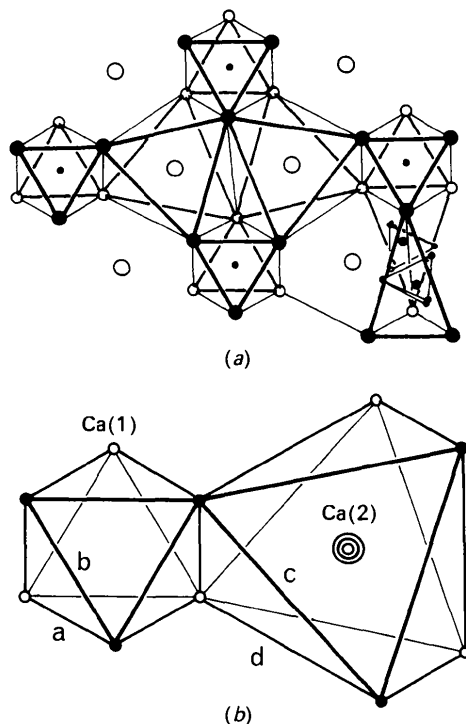

(a)

(b)

Fig. 3. (a) The Ca array in apatite projected onto the xy plane of the hexagonal unit cell, showing both the h.c.p. and the distorted b.c.c. blocks. Drawn on the lower-right-hand side are two PO_4 units inserted into the distorted Ca_4 tetrahedra. (b) Magnified view of one h.c.p. and one distorted b.c.c. Ca block, showing the Ca—Ca distances, $a = 4\cdot17$, $b = 4\cdot08$, $c = 6\cdot30$ and $d = 5\cdot83$ Å. Ca(1) atoms at $z = \frac{1}{4}, \frac{3}{4}$. Triple circle represents the three Ca(2) atoms at $z \simeq 0, \frac{1}{2}, 1$.

The Ca—Ca distances can justify our choice. In the h.c.p. octahedra these distances are 4·08 and 4·17 Å for the horizontal and sloping edges, respectively, so that these blocks are not solely ordered 'as in h.c.p.' [this is explicitly stated by O'Keeffe & Hyde, (1985)], nor are they solely Mg-like blocks, as stated by Schubert (1964), but are just h.c.p. calcium (Ca—Ca distance of 3·97 Å). In the distorted b.c.c.-like blocks, the Ca(1)—Ca(1) distances are 6·30 Å for the six horizontal edges and 5·83 and 4·17 Å for the sloping edges. The Ca(2) atom, at the body center, has six neighbours at 3·88 Å and two additional ones at 3·44 Å (mean value 3·77 Å). Compare these distances with those in b.c.c. calcium, where the central atom has eight neighbours at 3·88 Å and the corresponding octahedral horizontal edges are 6 × 6·33 Å. Although distortion exists, the b.c.c. identity of calcium is substantially preserved. The two regular triangles formed by the six face diagonals of the cube (c distances in Fig. 3b) and the distances from the body center to these six corners are the same (within 1–2%) as in b.c.c. calcium.

Distortion takes place by twisting these triangles with respect to each other, so as to attain the distances of 4·17 Å (a in Fig. 3b) which are common to the h.c.p. blocks. This also gives rise to a lengthening of the other sloping edges (d in Fig. 3b). These edges would correspond to the cube edge (4·48 Å) in b.c.c. calcium. Note that the twist just described occurs as if rigid triangles are pushed away by the PO_4 groups. However, the distortion could also be explained by the need to attain a distance (4·17 Å) which is a compromise between the distances of 4·48 and 3·97 Å for b.c.c. and h.c.p. calcium, respectively. In this way, the irregular Ca_4 tetrahedra that are generated would be big enough to include the PO_4 groups. We are not able to decide between the two explanations; we only know that two phases of calcium can be recognized in the apatite structure. Our view is coincident with that of Schubert (1964), but differs in that the Mg-like and β-W-like blocks are now recognized as two known phases of calcium.

β-Ca_2SiO_4 and hexagonal calcium

O'Keeffe & Hyde (1985) have shown that β-Ca_2SiO_4 is one of the compounds in which the cation array is the same as in the parent Ca_2Si alloy. The latter structure (Eckerlin & Wölfel, 1955) is represented in Fig. 4. It has been described as an Ni_2Si- or $PbCl_2$-like structure, formed by infinite chains of edge-sharing trigonal prisms. These chains are shifted relative to each other by $c/2$.

Our alternative view corresponds to a h.c.p. of Ca atoms, very distorted by the presence of Si atoms at the center of Ca_3 triangles (see Fig. 4), and just those capping the lateral faces of trigonal prisms. The

triangular faces of the prisms are again octahedral faces of a very distorted h.c.p. The Ca—Ca distances within them are 4·06, 3·75 and 3·61 Å, respectively (mean value of 3·81 Å, only 4% shorter than in hexagonal calcium, 3·97 Å). The other three horizontal edges are 4·99, 5·36 and 5·55 Å, the six sloping edges completing the distorted octahedron being in the range 3·57 to 4·01 Å.

This compound has a high-temperature modification, the olivine-like γ-phase (Czaya, 1971), which has already been discussed. As has been pointed out (O'Keeffe & Hyde, 1985), this transition is accompanied by an increase in the a parameter of the unit cell of the γ-phase, corresponding to a greater separation of the chains of trigonal prisms. Thus, it seems that the deformed h.c.p. of Ca atoms in the β-phase breaks down entirely in the olivine-like phase. In it, the corresponding distorted octahedra, defined by us in the β-phase, have sloping Ca—Ca distances in the range 3·89–4·28 Å.

Concluding remarks

The fact that some oxides show the same cation array as the parent element or alloy does not seem to be restricted to the few examples given before (O'Keeffe & Hyde, 1985). The results we have discussed suggest that the structural 'identity' of the parent metal can be detected in other compounds. The parent metal is recognized either in a distorted form or as fragments (variable in size and shape) of
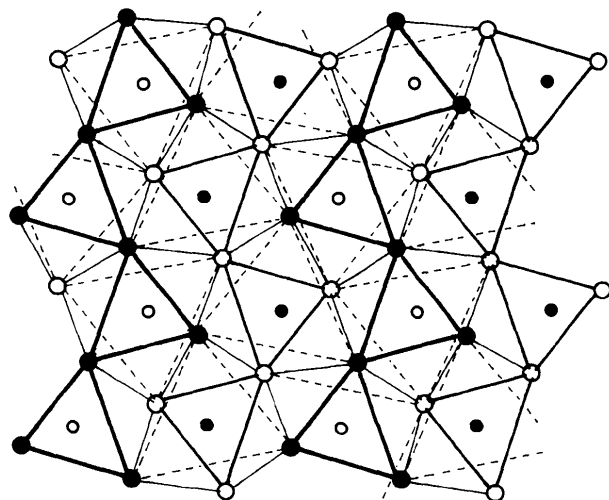
that original structure, which is broken down by the inclusion of other atoms or anions. In both cases, the cation–cation distances in oxides permit the identification of the parent metal structure.

We have previously given some examples (Vegas, 1985; Marcano, Rasines, Vegas & Otero-Diaz, 1987, 1988) of the usefulness of the 'cationic model' developed by O'Keeffe & Hyde (1985). However, we believe that the model we present has some advantages. Firstly, it seems to us that thinking of the minerals of the humite series (all of them Mg-containing borates and silicates) as being formed by different fragments of the common parent Mg, is more graphic than to describe them as intergrowths of such different compounds as CrB, Ni$_2$In and Re$_3$B. Secondly, it is possible that a metallic net does not necessarily need to be broken down completely into atoms to form a compound. Even if this were so, the impression is that the atoms partially recombine as they were before compound formation.

At present we cannot confirm the general applicability of these ideas. Indeed, further work is in progress to establish their limitations. However, they result from a search for new models which could be "more intuitive and have some physical feel" (Hyde, 1986) in the sense that Bragg, in 1914, described calcite as a deformed NaCl-like structure [see Megaw (1973)].

Finally, we are aware that we have dealt only with the *description* of crystal structures, without considering the important aspects of *explanation*. These concepts appear to be quite close, indeed quite difficult to separate, in the current structural context. We hope, however, that our ideas might contribute, even through the description, to a better understanding of how a given structure is formed, and to a visualization of what happens when crystals grow or what happens inside a crucible when solids react.

Fig. 4. The Ca$_2$Si structure projected onto the xz plane. Small and large circles are Si and Ca atoms, respectively (open at $y = \frac{1}{4}$, filled at $y = \frac{3}{4}$). Thin lines (dashed and continuous) define the deformed Ca$_6$ octahedra with Si atoms at the center of expanded Ca$_3$ triangles. Open circles ($y = \frac{1}{4}$) cap lateral faces of the Ca$_6$ trigonal prisms defined by four filled circles ($y = -\frac{1}{4}, \frac{3}{4}$) and *vice versa*.

References

BELOKONEVA, E. L., SIMONOV, M. A. & BELOV, N. V. (1973). *Sov. Phys. Dokl.* **17**, 1124–1125.

BROVKIN, A. A. & NIKISHOVA, L. V. (1975). *Sov. Phys. Crystallogr.* **20**, 252–254.

CZAYA, R. (1971). *Acta Cryst.* B**27**, 848–849.

ECKERLIN, P. & WÖLFEL, E. (1955). *Z. Anorg. Allg. Chem.* **280**, 321–331.

GIBBS, G. V. & RIBBE, P. H. (1969). *Am. Mineral.* **54**, 376–411.

GIBBS, G. V., RIBBE, P. H. & ANDERSON, C. P. (1970). *Am. Mineral.* **55**, 1182–1194.

HYDE, B. G. (1986). *J. Proc. R. Soc. NSW*, **119**, 153–164.

MARCANO, C. M., RASINES, I., VEGAS, A. & OTERO-DÍAZ, L. C. (1987). *Z. Anorg. Allg. Chem.* **555**, 176–182.

MARCANO, C. M., RASINES, I., VEGAS, A. & OTERO-DÍAZ, L. C. (1988). *Z. Anorg. Allg. Chem.* **561**, 192.

MEGAW, H. D. (1973). *Crystal Structures: A Working Approach*, p. 243. Philadelphia: W. B. Saunders.

NYMAN, H. & ANDERSSON, S. (1979). *Acta Cryst.* A35, 580–583.

O'KEEFFE, M. & HYDE, B. G. (1981). *Structure and Bonding in Crystals*, edited by M. O'KEEFFE and A. NAVROTSKY, ch. 10. New York: Wiley.

O'KEEFFE, M. & HYDE, B. G. (1985). *Struct. Bonding (Berlin)*, 61, 77–144.

RIBBE, P. H. & GIBBS, G. V. (1971). *Am. Mineral.* 56, 1155–1163.

ROBINSON, K., GIBBS, G. V. & RIBBE, P. H. (1973). *Am. Mineral.* 58, 43–49.

SCHUBERT, K. (1964). *Kristallstrukturen Zweikomponentiger Phasen*, pp. 305–307. Berlin: Springer Verlag.

SUDARSANAN, K. & YOUNG, R. A. (1969). *Acta Cryst.* B25, 1534–1543.

SUDARSANAN, K. & YOUNG, R. A. (1978). *Acta Cryst.* B43, 1401–1407.

VEGAS, A. (1985). *Acta Cryst.* C41, 1689–1690.

WENK, H. R. & RAYMOND, K. N. (1973). *Z. Kristallogr.* 137, 86–105.

WHITE, T. J. & HYDE, B. G. (1982a). *Phys. Chem. Miner.* 8, 55–63.

WHITE, T. J. & HYDE, B. G. (1982b). *Phys. Chem. Miner.* 8, 167–174.

WHITE, T. J. & HYDE, B. G. (1983). *Acta Cryst.* B33, 10–17.

WONDRATSCHEK, H., MERKER, L. & SCHUBERT, K. (1964a). *Z. Kristallogr.* 120, 393–395.

WONDRATSCHEK, H., MERKER, L. & SCHUBERT, K. (1964b). *Z. Kristallogr.* 120, 478.

ZEMANN, J., EFFENBERGER, H. & PERTLIK, F. (1982). *Österr. Akad. Wiss. Anzeig.* pp. 61–62.

Crystallization and Preliminary Structure Analysis of an Insect Virus with $T = 4$ Quasi-Symmetry: *Nudaurelia capensis* ω Virus

BY JEAN CAVARELLI,* WU BOMU,† LARS LILJAS,‡ SANGSOO KIM,§ WLADEK MINOR, SANJEEV MUNSHI, STEVE MUCHMORE, TIM SCHMIDT AND JOHN E. JOHNSON¶

Department of Biological Sciences, Purdue University, West Lafayette, Indiana 47907, USA

AND DONALD A. HENDRY

Department of Microbiology, Rhodes University, Grahamstown, 6140 South Africa

(*Received 14 March 1990; accepted 15 August 1990*)

Abstract

We report the crystallization of *Nudaurelia capensis* ω virus, a pathogen of the pine emperor moth. The icosahedral particle has $T = 4$ quasi-equivalent symmetry and is approximately 410 Å in diameter. Triclinic crystals ($a = 414\cdot0$, $b = 410\cdot7$, $c = 420\cdot1$ Å, $\alpha = 59\cdot1$, $\beta = 58\cdot9$, $\gamma = 64\cdot0°$) diffracting X-rays to 2·7 Å resolution have been analyzed using a partial data set collected at high resolution (2·7 Å) using conventional oscillation photography and a more complete data set collected at low resolution (50–9 Å) using a Siemens area detector. The pseudo-rhombohedral symmetry of the crystals created significant problems in processing the unaligned oscillation photographs. Successful processing of the films depended on the use of an auto-indexing procedure followed by systematic scaling tests of four, nearly equivalent, reduced cells. The unique cell from the area-detector data collection was identified by scaling the four possible choices with the film data. The particle orientation was determined using the rotation function.

Introduction

Nudaurelia capensis ω virus (NωV) is a spherical RNA virus that was first isolated from larvae of the pine emperor moth (Hendry, Hodgson, Clark & Newman, 1985). The virus has been isolated only from larvae infected in the wild and it has not been successfully propagated in insect cell lines. NωV particles appear spherical in the electron microscope with an estimated diameter of 410 Å. The capsid consists of multiple copies of a protein subunit of molecular weight 65 kD. The particles contain two RNA molecules with molecular weights of about 2·3 and 0·8 mD. The physical and biological properties of NωV classify it as a member of the family Tetraviridae whose prototype is *Nudaurelia capensis* β virus (NβV). Although NωV and NβV are both

* Present address: Laboratoire de Cristallographie Biologique, IBMC, CNRS, 15 rue Rene Descartes, 67084 Strasbourg, CEDEX, France.

† Present address: Institute of Biophysics, Academia Sinica, Beijing 100080, People's Republic of China.

‡ Permanent address: Department of Molecular Biology, University of Uppsala Biomedical Center, S-751 24 Uppsala, Sweden.

§ Present address: Lucky Central Research Institute, Science Town, PO Box 10, Dae Jeon, Chung-Nam, Korea.

¶ Author to whom correspondence should be addressed.